Legends for figures:

Fig. 1 The experimental schedule.

Fig. 2 TNF-α is required for the iNOS-mediated nitration of proteins and impairment of memory induced by $A\beta_{25-35}$. At different time points after the *i.c.v.*-injection of $A\beta_{25-35}$ (Day 0) in mice, the mRNA expression levels of TNF-α and iNOS in the hippocampus were investigated by using real-time RT-PCR. A: $A\beta_{25-35}$ induced a sharp increase of TNF-α and iNOS mRNA in two hours after injection, the expression of the former was stronger than that of the latter. Data were presented as the mean ± S.E. (n=4). * p <0.05 vs. control. B: TNF-α (-/-) prevented the increase of iNOS mRNA which was induced by $A\beta_{25-35}$ in WT mice. Data were presented as the mean ± S.E. (n=4). * p <0.05 vs. control. C-D: Either the selective inhibition of iNOS activity by AG or TNF-α (-/-) prevented the $A\beta_{25-35}$-induced nitration of proteins in the hippocampus (Day 7) and the impairment of novel object recognition memory (Day 8-10). Data were presented as the mean ± S.E., (n=4 for C, n=10 for D), *p <0.05 vs. control, $^{\#}p$ <0.05 vs. $A\beta_{25-35}$; TNF-α: tumor necrosis factor-alpha; iNOS: inducible nitric oxide synthase; WT: wild type; TNF-α (-/-): TNF-α knock out; AG: aminoguanidine; $A\beta_{25-35}$: Amyloid beta peptide (25-35).

Fig. 3 Thalidomide suppressed the increase of TNF-α mRNA induced by $A\beta_{1-40}$. Thalidomide (20mg/kg) was administrated *p.o.* one hour before the *i.c.v.*-injection of $A\beta_{1-40}$ in mice. A-D: Two hours after the injection of $A\beta_{1-40}$, the mRNA levels of TNF-α, iNOS, BDNF,

and GDNF in the hippocampus were investigated by using real-time RT-PCR. Thalidomide suppressed the increase of TNF-α and iNOS mRNA induced by $A\beta_{1-40}$. The mRNA levels of BDNF and GDNF in the hippocampus were not changed either by $A\beta_{1-40}$ injection or thalidomide treatment. Data were presented as the mean ± S.E., n=4, $^{*}p$ <0.05 vs. control, $^{\#}p$ <0.05 vs. $A\beta_{1-40}$; TNF-α: tumor necrosis factor-alpha; iNOS: inducible nitric oxide synthase; GDNF: glial cell-derived neurotrophic factor; BDNF: brain-derived neurotrophic factor; $A\beta_{1-40}$: Amyloid beta peptide (1-40). DMSO: dimethyl sulfoxide.

Fig. 4 Thalidomide prevented the nitration of proteins and the impairment of memory induced by Aβ. A-B: Thalidomide (20mg/kg) was administrated *p.o.* daily until Day 3 after the *i.c.v.*-injection of $A\beta_{25-35}$ or $A\beta_{1-40}$ (Day 0). An anti-TNF-α antibody (α-TNF-α) (10ng/mouse) was *i.c.v.*-injected 15 minutes prior to the injection of $A\beta_{25-35}$ or $A\beta_{1-40}$. Either the daily treatment with thalidomide or the *i.c.v.*-injection of α-TNF-α antibody prevented the nitration of proteins in the hippocampus (Day 7) and the impairment of novel object recognition memory (Day 8-10) induced by $A\beta_{25-35}$ or $A\beta_{1-40}$. Data were presented as the mean ± S.E., (n=4 for E, n=10 for F), $^{*}p$ <0.05 vs. control; $^{\#}p$ <0.05 vs. $A\beta_{25-35}$ or $A\beta_{1-40}$; α-TNF-α: anti-TNF-α antibody; $A\beta_{35-25}$: Amyloid beta peptide (35-25). $A\beta_{1-40}$: Amyloid beta peptide (1-40).

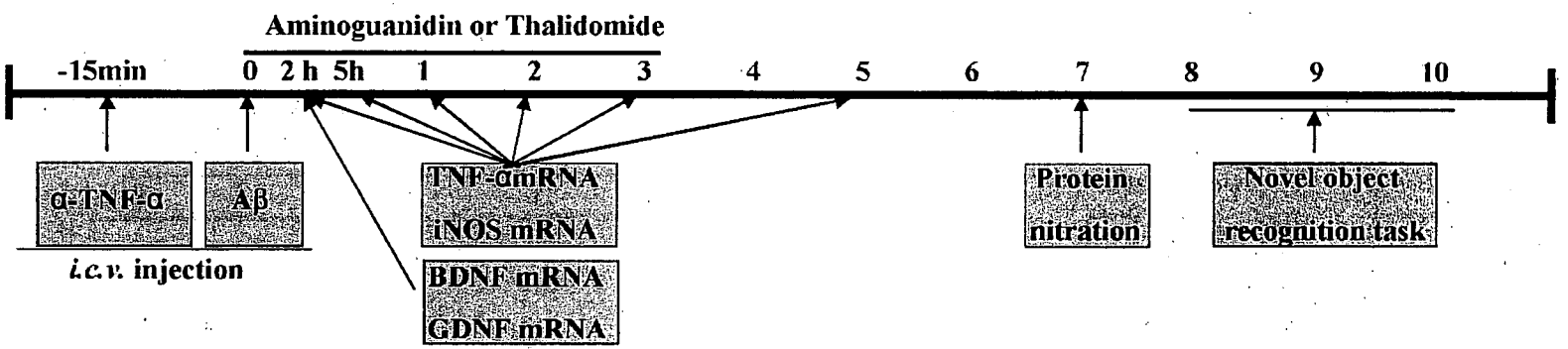

Fig. 1

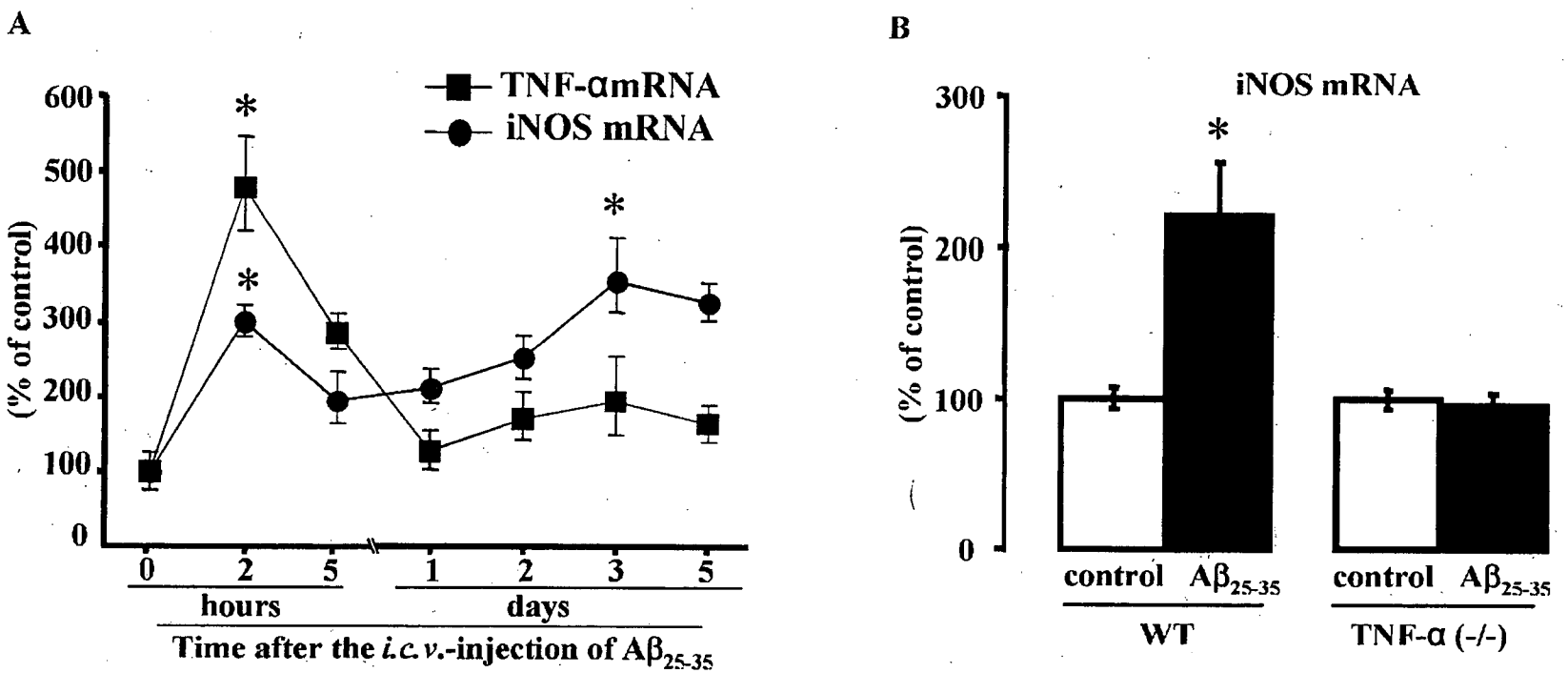
A
TNF-αmRNA
iNOS mRNA
600
500
400
300
200
100
0
(% of control)
*
*
*
0
2
5
1
2
3
5
hours
days
Time after the i.c.v.-injection of Aβ25-35
B
iNOS mRNA
300
200
100
0
(% of control)
*
control
Aβ25-35
control
Aβ25-35
WT
TNF-α (-/-)

Fig. 2-1

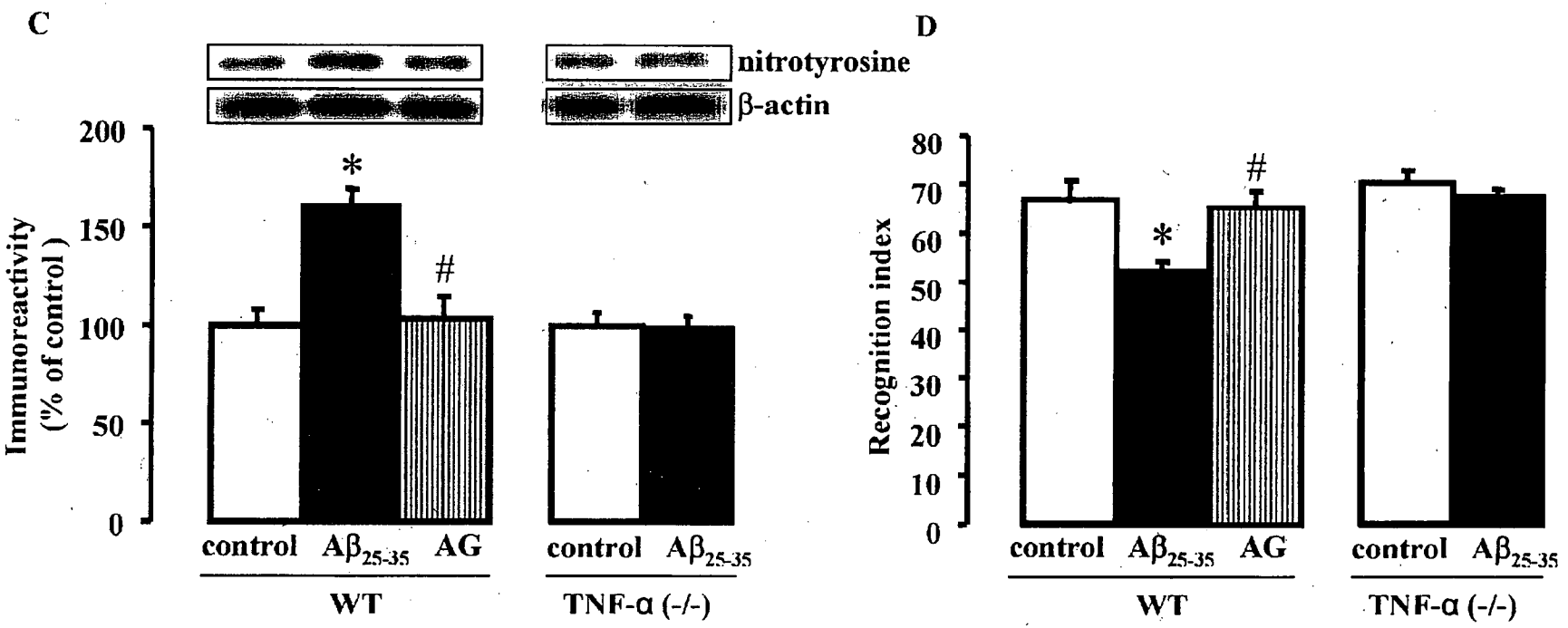
C
nitrotyrosine
β-actin
Immunoreactivity (% of control)
200
150
100
50
0
*
#
control
Aβ25-35
AG
control
Aβ25-35
WT
TNF-α (-/-)
D
Recognition index
80
70
60
50
40
30
20
10
0
*
#
control
Aβ25-35
AG
control
Aβ25-35
WT
TNF-α (-/-)

Fig. 2-2

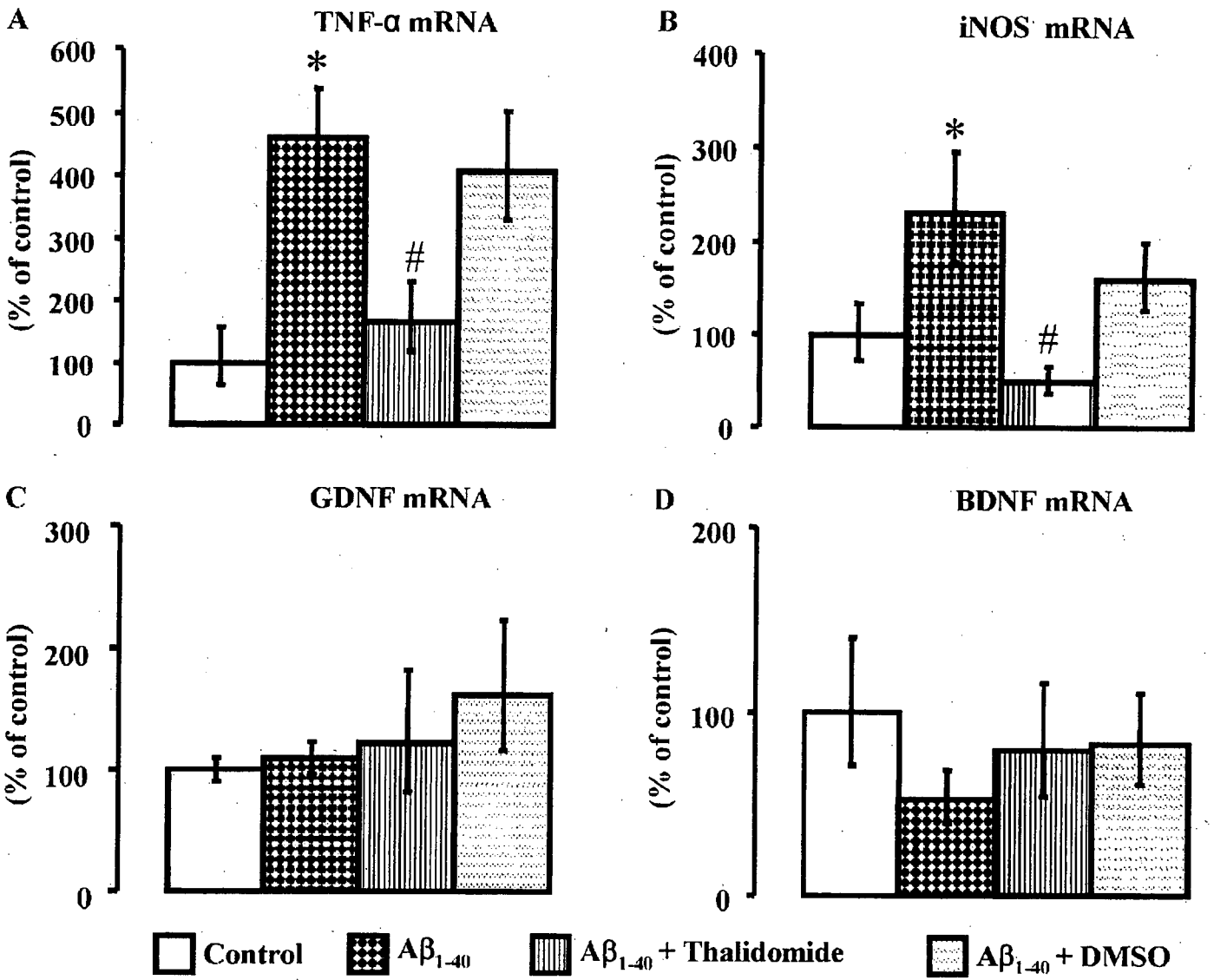
A
TNF-α mRNA
(% of control)
600
500
400
300
200
100
0
*
#
B
iNOS mRNA
(% of control)
400
300
200
100
0
*
#
C
GDNF mRNA
(% of control)
300
200
100
0
D
BDNF mRNA
(% of control)
200
100
0
Control
Aβ1-40
Aβ1-40 + Thalidomide
Aβ1-40 + DMSO

Fig. 3

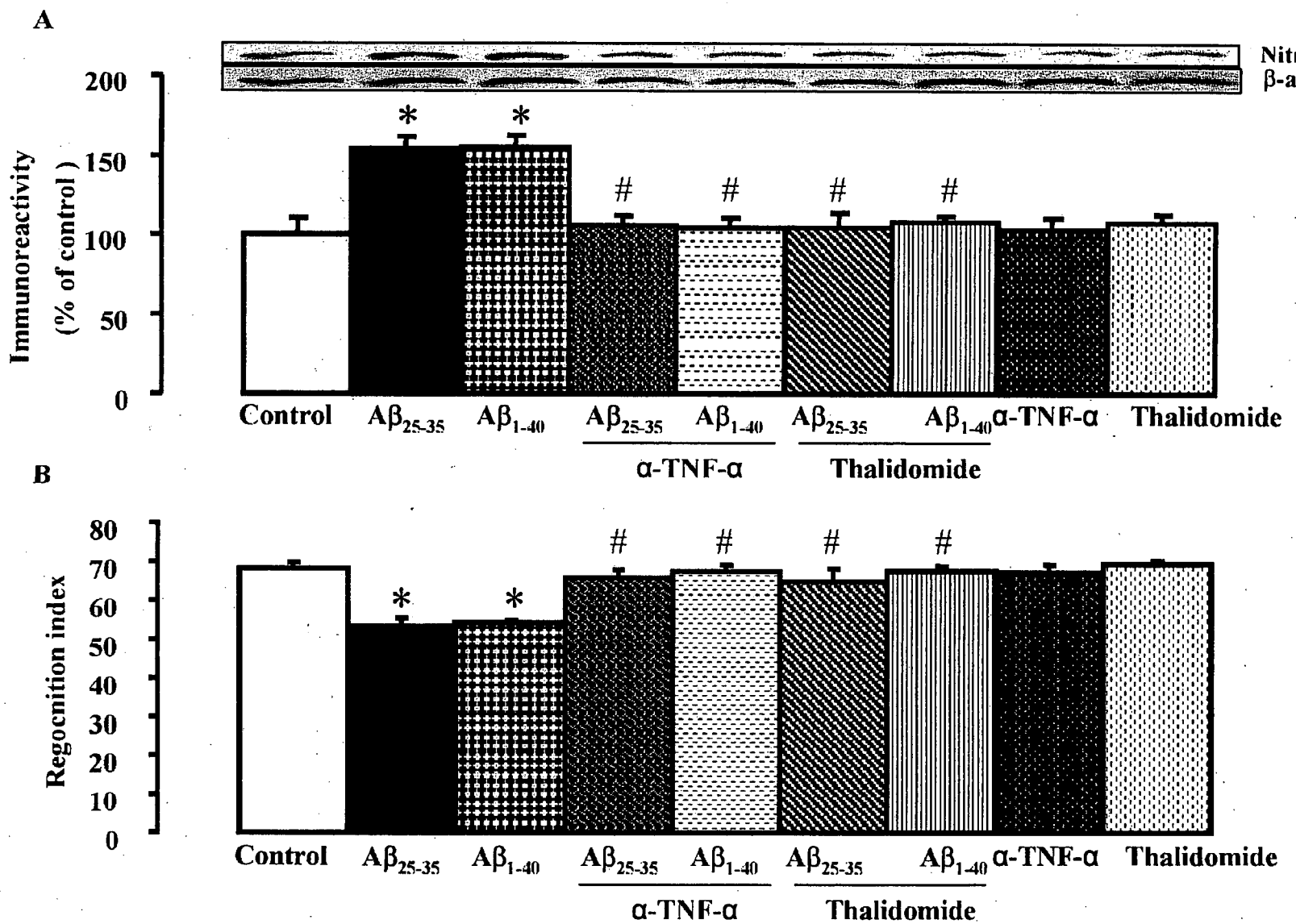

Fig. 4

Pollock, J.S., Forstermann, U., Mitchell, J.A., Warner, T.D., Schmidt, H.H.H.W., Nakane, M., Murad, F., 1991. Purification and characterization of particulate endothelium-derived relaxing factor synthase from cultured and native bovine aortic endothelial cells. Proc. Natl. Acad. Sci. 88, 10480–10484.

Röhn, T.A., Jennings, G.T., Hernandez, M., Grest, P., Beck, M., Zou, Y., Kopf, M., Bachmann, M.F., 2006. Vaccination against IL-17 suppresses autoimmune arthritis and encephalomyelitis. Eur. J. Immunol. 36 (11), 2844–2848.

Sonobe, Y., Yawata, I., Kawanokuchi, J., Takeuchi, H., Mizuno, T., Suzumura, A., 2005. Production of IL-27 and other IL-12 family cytokines by microglia and their subpopulations. Brain Res. 1040 (1–2), 202–207.

Suzumura, A., Mezitis, S.G., Gonatas, N.K., Silberberg, D.H., 1987. MHC antigen expression on bulk isolated macrophage-microglia from newborn mouse brain: induction of Ia antigen expression by gamma-interferon. J. Neuroimmunol. 15 (3), 263–278.

Suzumura, A., Takeuchi, H., Zhang, G., Kuno, R., Mizuno, T., 2006. Roles of glia-derived cytokines on neuronal degeneration and regeneration. Ann. N. Y. Acad. Sci. 1088, 219–229 Review.

Takeuchi, H., Mizuno, T., Zhang, G., Wang, J., Kawanokuchi, J., Kuno, R., Suzumura, A., 2005. Neuritic beading induced by activated microglia is an early feature of neuronal dysfunction toward neuronal death by inhibition of mitochondrial respiration and axonal transport. J. Biol. Chem. 280 (11), 10444–10454.

Towbin, H., Staehelin, T., Gordon, J., 1979. Electrophoretic transfer of proteins from polyacrylamide gels to nitrocellulose sheets: procedure and some applications. Proc. Natl. Acad. Sci. U. S. A. 76 (9), 4350–4354.

Trajkovic, V., Stosic-Grujicic, S., Samardzic, T., Markovic, M., Miljkovic, D., Ramic, Z., MostraricaStojkovic, M., 2001. Interleukin-17 stimulates inducible nitric oxide synthase activation in rodent astrocytes. J. Neuroimmunol. 119, 183–191.

Valdhoen, M., Hocking, R.J., Atkins, C.J., Locksley, R.M., Stockinger, B., 2006. TGFbeta in the context of an inflammatory cytokine milieu supports de novo differentiation of IL-17 producing T cells. Immunity 24, 179–189.

Yao, Z., Painter, S.L., Fanslow, W.C., Ulrich, D., Macduff, B.M., Spriggs, M.K., Armitage, R.J., 1995. Human IL-17: a novel cytokine derived from T cells. J. Immunol. 155 (12), 5483–5486.

Please cite this article as: Kawanokuchi, J., et al., Production and functions of IL-17 in microglia, J. Neuroimmunol. (2007), doi:10.1016/j.jneuroim.2007.11.006

vaccination against IL-17 may therefore be an attractive therapeutic alternative, which could allow more patients access to an effective therapy that acts at an earlier stage of disease.

Acknowledgments

This work was supported in part by a Grant-in-Aid for Scientific Research and for the Creation of Innovations through the Business-Academic-Public Sector Cooperation from the Ministry of Education, Culture, Sports, Science and Technology of Japan as well as a Grant-in-Aid for Medical Frontier Strategy Research and for Research on Intractable Diseases from the Japanese Ministry of Health, Labour and Welfare. This work was also supported by the 21st COE Program "Integrated Molecular Medicine for Neuronal and Neoplastic Disorders" from the Ministry of Education, Culture, Sports, Science and Technology.

References

Aggarwal, S., Gurney, A.L., 2002. IL-17: prototype member of an emerging cytokine family. J. Leukoc. Biol. 71, 1–8.

Aggarwal, S., Ghilardi, N., Xie, M.H., de Sauvage, F.J., Gurney, A.L., 2003. Interleukin-23 promotes a distinct CD4 T cell activation state characterized by the production of interleukin-17. J. Biol. Chem. 278 (3), 1910–1914.

Batten, M., Li, J., Yi, S., Kljavin, N.M., Danilenko, D.M., Lucas, S., Lee, J., de Sauvage, F.J., Ghilardi, N., 2006. Interleukin 27 limits autoimmune encephalomyelitis by suppressing the development of interleukin 17-producing T cells. Nat. Immunol. 7, 929–936.

Bessis, A., Bechade, C., Bernard, D., Roumier, A., 2007. Microglial control of neuronal death and synaptic properties. Glia 55 (3), 233–238 Review.

Bettelli, E., Carrier, Y., Gao, W., Korn, T., Strom, T.B., Oukka, M., Weiner, H.L., Kuchroo, V.K., 2006. Reciprocal developmental pathways for the generation of pathogenic effector TH17 and regulatory T cells. Nature 441 (7090), 235–238.

Cai, X.Y., Gommoll Jr., C.P., Justice, L., Narula, S.K., Fine, J.S., 1998. Regulation of granulocyte colony-stimulating factor gene expression by interleukin-17. Immunol. Lett. 62, 51–58.

Chabaud, M., Fossiez, F., Taupin, J.L., Miossec, P., 1998. Enhancing effect of IL-17 on IL-1-induced IL-6 and leukemia inhibitory factor production by rheumatoid arthritis synoviocytes and its regulation by Th2 cytokines. J. Immunol. 161, 409–414.

Chen, Y., Langrish, C.L., McKenzie, B., Joyce-Shaikh, B., Stumhofer, J.S., McClanahan, T., Blumenschein, W., Churakovsa, T., Low, J., Presta, L., Hunter, C.A., Kastelein, R.A., Cua, D.J., 2006. Anti-IL-23 therapy inhibits multiple inflammatory pathways and ameliorates autoimmune encephalomyelitis. J. Clin. Invest. 116 (5), 1317–1326.

Fossiez, F., Djossou, O., Chomarat, P., Flores-Romo, L., Ait-Yahia, S., Maat, C., Pin, J.J., Garrone, P., Garcia, E., Saeland, S., Blanchard, D., Gaillard, C., Das, M.B., Rouvier, E., Golstein, P., Banchereau, J., Lebecque, S., 1996. T cell interleukin-17 induces stromal cells to produce proinflammatory and hematopoietic cytokines. J. Exp. Med. 183, 2593–2603.

Furukawa, S., Kamo, I., Furukawa, Y., Akazawa, S., Satoyoshi, E., Itoh, K., Hayashi, K., 1983. A highly sensitive enzyme immunoassay for mouse beta nerve growth factor. J. Neurochem. 40, 734–744.

Harrington, L.E., Hatton, R.D., Mangan, P.R., Turner, H., Murphy, T.L., Murphy, K.M., Weaver, C.T., 2005. Interleukin 17-producing $CD4^+$ effector T cells develop via a lineage distinct from the T helper type 1 and 2 lineages. Nat. Immunol. 6 (11), 1123–1132.

Hofstetter, H.H., Ibrahim, S.M., Koczan, D., Kruse, N., Weishaupt, A., Toyka, K.V., Gold, R., 2005. Therapeutic efficacy of IL-17 neutralization in murine experimental autoimmune encephalomyelitis. Cell Immunol. 237 (2), 123–130.

Ignarro, L.J., Buga, G.M., Wood, K.S., Byrns, R.E., Chaudhuri, G., 1987. Endothelium-derived relaxing factor produced and released from artery and vein in nitric oxide. Proc. Natl. Acad. Sci. USA, 84, 9265–9269.

Ishizu, T., Osoegawa, M., Mei, F.J., Kikuchi, H., Tanaka, M., Takakura, Y., Minohara, M., Murai, H., Mihara, F., Taniwaki, T., Kira, J., 2005. Intrathecal activation of the IL-17/IL-8 axis in opticospinal multiple sclerosis. Brain 128, 988–1002.

Ivanov, I.I., McKenzie, B.S., Zhou, L., Tadokoro, C., Lepelley, A., Lafaille, J., Cua, D., Littman, D., 2006. The orphan nuclear receptor RORgammat directs the differentiation program of proinflammatory $IL\text{-}17^+$ T helper cells. Cell 126, 1121–1133.

Iwakura, Y., Ishigame, H., 2006. The IL-23/IL-17 axis in inflammation. J. Clin. Invest. 116 (5), 1218–1922.

Jovanovic, D.V., Di, B.J.A., Martel-Pelletier, J., Jolicoeur, F.C., He, Y., Zhang, M., Mineau, F., Pelletier, J.P., 1998. IL-17 stimulates the production and expression of proinflammatory cytokines, IL-b and TNFa, by human macrophages. J. Immunol. 160, 3513–3521.

Kaechi, K., Furukawa, Y., Ikegami, R., Nakamura, N., Omae, F., Hashimoto, Y., Hayashi, K., Furukawa, S., 1993. Pharmacological induction of physiologically active nerve growth factor in rat peripheral nervous system. J. Pharmacol. Exp. Ther. 264, 321–326.

Kennedy, J., Rossi, D.L., Zurawski, S.M., Vega Jr., F., Kastelein, R.A., Wagner, J.L., Hannum, C.H., Zlotnik, A., 1996. Mouse IL-17: a cytokine preferentially expressed by alpha beta $TCR+CD4^-CD8^-$ T cells. J. Interferon Cytokine Res. 16, 611–617.

Komiyama, Y., Nakae, S., Matsuki, T., Nambu, A., Ishigame, H., Kakuta, S., Sudo, K., Iwakura, Y., 2006. IL-17 plays an important role in the development of experimental autoimmune encephalomyelitis. J. Immunol. 177, 566–573.

Kuno, R., Yoshida, Y., Nitta, A., Nabeshima, T., Wang, J., Sonobe, Y., Kawanokuchi, J., Takeuchi, H., Mizuno, T., Suzumura, A., 2006. The role of TNF-alpha and its receptors in the production of NGF and GDNF by astrocytes. Brain Res. 1116 (1), 12–18.

Laan, M., Cui, Z.H., Hoshino, H., Lotvall, J., Sjostrand, M., Gruenert, D.C., Skoogh, B.E., Linden, A., 1999. Neutrophil recruitment by human IL-17 via C–X–C chemokine release in the airways. J. Immunol. 162, 2347–2352.

Laemmli, U.K., Favre, M., 1973. Maturation of the head of bacteriophage T4. I. DNA packaging events. J. Mol. Biol. 80 (4), 575–579.

Li, G.Z., Zhong, D., Yang, L.M., Sun, B., Zhong, Z.H., Yin, Y.H., Cheng, J., Yan, B.B., Li, H.L., 2005. Expression of interleukin-17 in ischemic brain tissue. Scand. J. Immunol. 62 (5), 481–486.

Li, Y., Chu, N., Hu, A., Gran, B., Rostami, A., Zhang, G.X., 2007. Increased IL-23p19 expression in multiple sclerosis lesions and its induction in microglia. Brain 130 (Pt2), 490–501.

Linden, A., Hoshino, H., Laan, M., 2000. Airway neutrophils and interleukin-17. Eur. Respir. J. 15, 973–977.

Lock, C., Hermans, G., Pedotti, R., Brendolan, A., Schadt, E., Garren, H., Langer-Gould, A., Strober, S., Cannella, B., Allard, J., Klonowski, P., Austin, A., Lad, N., Kaminski, N., Galli, S.J., Oksenberg, J.R., Raine, C.S., Heller, R., Steinman, L., 2003. Gene-microarray analysis of multiple sclerosis lesions yields new targets validated in autoimmune encephalomyelitis. Nat. Med. 8 (5), 500–208.

Matusevicius, D., Kivisakk, P., He, B., Kostulas, N., Ozenci, V., Fredrikson, S., Link, H., 1999. Interleukin-17 mRNA expression in blood and CSF mononuclear cells is augmented in multiple sclerosis. Mult. Scler. 5 (2), 101–104.

Meeuwsen, S., Persoon-Deen, C., Bsibsi, M., Ravid, R., van Noort, J.M., 2003. Cytokine, chemokine and growth factor gene profiling of cultured human astrocytes after exposure to proinflammatory stimuli. Glia 43 (3), 243–253.

Nitta, A., Ito, M., Fukumitsu, H., Ohmiya, M., Ito, H., Sometani, A., Nomoto, H., Furukawa, Y., Furukawa, S., 1999. 4-methylcatechol increases brain-derived neurotrophic factor content and mRNA expression in cultured brain cells and in rat brain in vivo. J. Pharmacol. Exp. Ther. 291, 1276–1283.

Nitta, A., Nishioka, H., Fukumitsu, H., Furukawa, Y., Sugiura, H., Shen, L., Furukawa, S., 2004. Hydrophobic dipeptide Leu-Ile protects against neuronal death by inducing brain-derived neurotrophic factor and glial cell line-derived neurotrophic factor synthesis. J. Neurosci. Res. 78, 250–258.

Park, H., Li, Z., Yang, X.O., Chang, S.H., Nurieva, R., Wang, Y.H., Wang, Y., Hood, L., Zhu, Z., Tian, Q., Dong, C., 2005. A distinct lineage of CD4 T cells regulates tissue inflammation by producing interleukin 17. Nat. Immunol. 6 (11), 1133–1141.

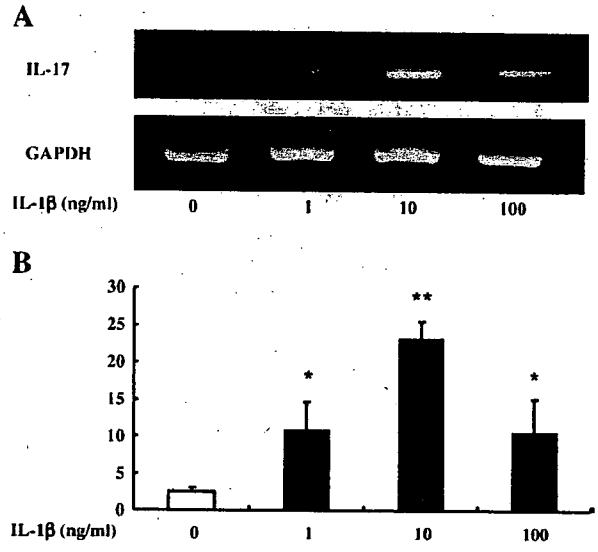

Fig. 8. IL-1β induces IL-17 production by microglia. Microglia were stimulated with various concentrations of IL-1β for 72 h. IL-1β induced IL-17 mRNA expression (A) and increased cytoplasmic IL-17 levels in microglia (B). The values shown are the means±S.D. $*P<0.05$ and $**P<0.01$ compared with untreated microglia. The data represent typical samples performed in triplicate in three independent experiments.

production in unstimulated microglia or in IL-23-stimulated microglia (data not shown). Stimulation with both IL-6 (100 ng/ml) and TGF-β (10 ng/ml) also failed to enhance the level of IL-17 produced by IL-23-stimulated microglia (data not shown).

4. Discussion

IL-17 has been associated with various autoimmune diseases, although its regulation and functional roles remain to be clarified. Antibodies specific for IL-17 reportedly inhibit chemokine expression in the brain during EAE, whereas overexpression of IL-17 in lung epithelia results in chemokine production and leukocyte infiltration. Thus, IL-17 expression characterizes a unique T helper lineage that regulates tissue inflammation (Park et al., 2005). Here we have evaluated the effects of IL-17 on neural cells *in vitro*. In the CNS, microglia and astrocytes express IL-17 receptors, whereas neurons do not. We then examined the effects of IL-17 on microglia—the antigen-presenting effector cells that can induce autoimmune inflammatory processes in the CNS. Because both IL-4 and IFNγ negatively regulate the production of IL-17 by T helper cells during the effector phase, Th17 cells may have roles that are distinct from those of Th1 and Th2 cells. The effects of IL-17 on microglia, however, are similar to those of Th1 cytokines; IL-17 enhanced inflammatory cytokine and chemokine production by microglia. IL-17 did not affect IFNγ-induced MHC class II antigen expression by microglia, whereas it increased the IFNγ-induced expression of adhesion molecules by these cells. IL-17 by itself did not induce iNOS expression or NO production, although it enhanced both of these phenomena in LPS-stimulated microglia. In rodent astrocytes, it has been shown that IL-17 enhances IFNγ-induced iNOS expression, which is suppressed by inhibitors of NF-κB or p38 MAP kinase (Trajkovic et al., 2001). Thus, IL-17 functions as a proinflammatory cytokine that works synergistically with other inflammatory stimuli in the CNS.

In addition to the proinflammatory effects on microglia, IL-17 also enhanced the expression of neurotrophic factors by microglia. We and other groups have previously shown that proinflammatory cytokines or inflammatory stimuli induce the expression of neurotrophic factors in microglia (Suzumura et al., 2006; Bessis et al., 2007). This may contribute to anti-inflammatory defense mechanisms in the CNS and implies that microglia may have multiple functions.

Previous cDNA microarray and immunohistochemical studies have suggested that astrocytes produce IL-17 (Meeuwsen et al., 2003; Li et al., 2005). In this study, we showed for the first time that microglia produce IL-17 in response to IL-23 or IL-1β. Although IL-1β and IL-23 induced IL-17 mRNA expression in microglia, we did not detect IL-17 in the supernatant of these cells. It is possible that IL-1β and IL-23 stimulate microglia to produce very low amount of IL-17 that cannot be detected with a commercially available ELISA kit, or that microglia may require another stimulatory signal before they release IL-17.

The same stimulus, however, did not induce the expression of IL-17 mRNA and protein in astrocytes. Thus, other stimuli may induce astrocytes to produce IL-17. Alternatively, this result may be due to differences between the species. As we and other groups have shown, IL-1β and IL-23 are produced by microglia in the CNS (Sonobe et al., 2005; Suzumura et al., 2006; Li et al., 2007). Therefore, it is possible that IL-1β and IL-23 may function as autocrine mediators that induce IL-17 expression by microglia.

Both Th1 and Th2 cytokines negatively regulate the differentiation of IL-17-producing T cells (Iwakura and Ishigame, 2006). In contrast, recent studies suggest that TGF-β derived from regulatory T cells induces an upregulation of IL-23 receptor expression and differentiation of Th17 cells in the presence of IL-6 (Ivanov et al., 2006; Valdhoen et al., 2006). Neither TGF-β nor IL-6, however, affects IL-17 production in microglia. Treatment of IL-23-stimulated microglia with both TGF-β and IL-6 also failed to enhance IL-17 production. These results suggest that different regulatory mechanisms control IL-17 production in microglia and Th17 cells.

Microglia play a pivotal role in the pathogenesis of inflammatory autoimmune diseases in the CNS. Thus, therapeutic targeting of the microglial production of IL-17 might be a useful strategy to treat MS. Because IL-17 deficiency has been demonstrated to ameliorate EAE in mice (Komiyama et al., 2006), induction of neutralizing antibodies that target the IL-23/IL-17 immune axis in microglia may provide a novel therapeutic approach for the treatment of MS. Indeed, targeting IL-23 with neutralizing antibodies ameliorates EAE and reduces serum levels of IL-17 (Chen et al., 2006). Moreover, a previous study demonstrated that blocking IL-17 with neutralizing antibodies induced by an active vaccination efficiently delays the onset of disease and reduces the severity of EAE (Röhn et al., 2006). Inflammatory autoimmune diseases such as MS, however, are chronic in nature, and treatment of these diseases with autoantibodies is extremely costly. Active

Please cite this article as: Kawanokuchi, J. et al., Production and functions of IL-17 in microglia, J. Neuroimmunol. (2007), doi:10.1016/j.jneuroim.2007.01.006

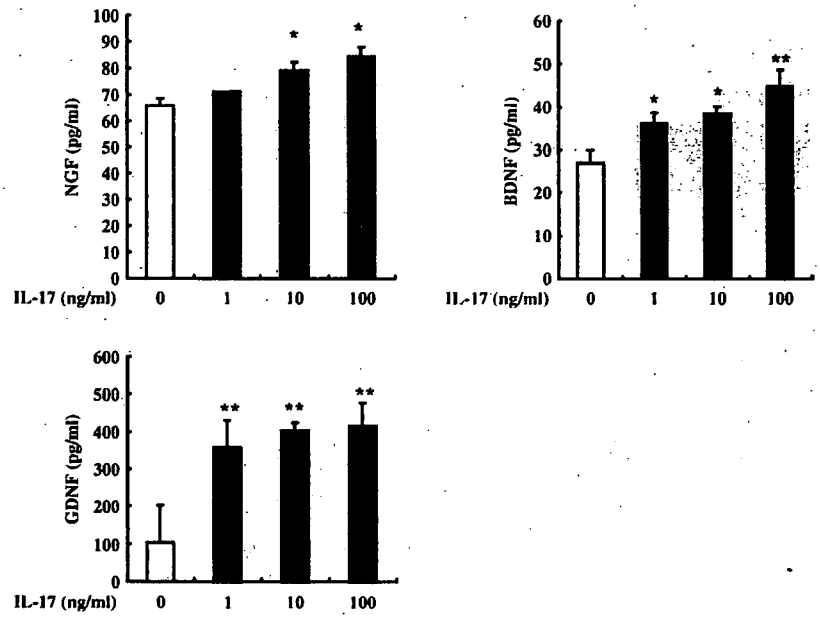

Fig. 5. The effects of IL-17 on the expression of neurotrophic factors in microglia. Microglia were treated with IL-17 for 72 h. IL-17 dose-dependently induced the expression of NGF, BDNF, and GDNF. The values shown are the means±S.D. $*P<0.05$ and $**P<0.01$ compared with untreated microglia. The data represent typical samples performed in triplicate in three independent experiments.

3.3. Production of IL-17 by microglia

IL-17 is reported to be a T cell-specific cytokine (Yao et al., 1995). A study that analyzed human astrocytes using cDNA microarrays, however, suggested that CNS cells produce IL-17 (Meeuwsen et al., 2003). Thus, we assessed IL-17 production in glial cells. Although unstimulated microglia did not express mRNA coding for IL-17, IL-23 induced IL-17 mRNA expression in microglia in a dose-dependent manner. Because ELISAs failed to detect IL-17 in the supernatant of IL-23-stimulated microglia, we measured the cytoplasmic levels of IL-17 in IL-23-stimulated microglia. IL-23 (≥1 ng/ml) significantly increased the cytoplasmic level of IL-17 in a dose-dependent manner (Fig. 7). IL-1β (≥1 ng/ml) also induced the expression of IL-17 mRNA and increased the cytoplasmic level of IL-17 in microglia; maximum induction was observed at 10 ng/ml (Fig. 8). On the contrary, stimulation with IL-23 or IL-23 and IL-1β did not induce IL-17 mRNA expression in astrocytes (data not shown). In the presence of IL-6, TGF-β derived from regulatory T cells induces upregulation of IL-23 receptor expression in Th17 cells (Ivanov et al., 2006). Neither IL-6 nor TGF-β, however, enhanced IL-17

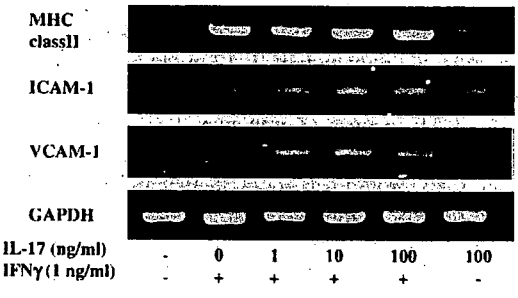

Fig. 6. The effects of IL-17 on the expression of mRNA encoding MHC antigen and adhesion molecules. Microglia were stimulated with IFNγ for 48 h in the presence of various concentrations of IL-17. IL-17 enhanced ICAM-1 and VCAM-1 mRNA expression in INFγ-stimulated microglia, whereas it did not affect MHC class II antigen mRNA levels in these cells.

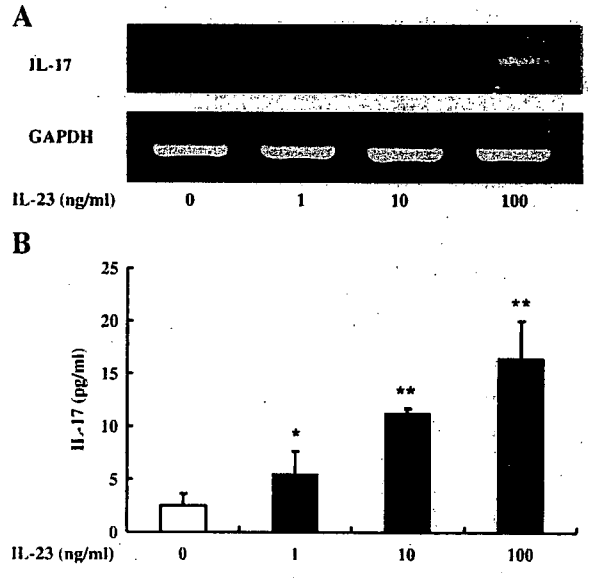

Fig. 7. IL-23 induces IL-17 production by microglia. Microglia were stimulated with various concentrations of IL-23 for 72 h. IL-23 dose-dependently induced IL-17 mRNA expression (A) and increased cytoplasmic IL-17 levels in microglia (B). The values shown are the means±S.D. $*P<0.05$ and $**P<0.01$ compared with untreated microglia. The data represent typical samples performed in triplicate in three independent experiments.

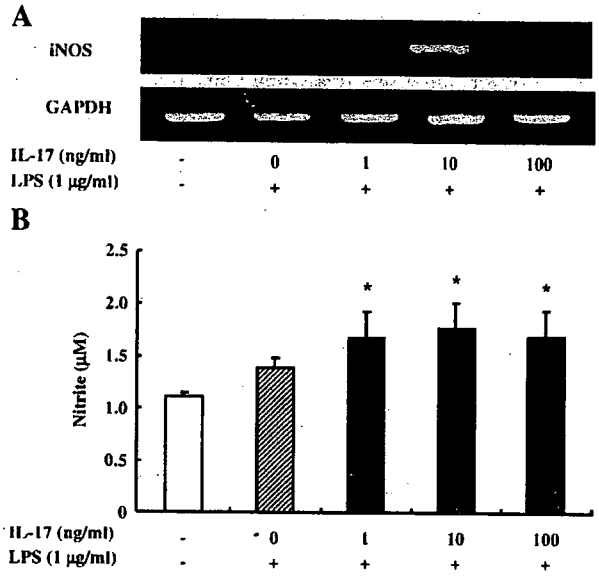

Fig. 3. The effects of IL-17 on NO production and iNOS expression in LPS-stimulated microglia. Microglia were stimulated with LPS for 48 h in the presence of various concentrations of IL-17. IL-17 enhanced iNOS mRNA expression (A) and NO production (B). The values shown are the means±S.D. $*P<0.05$ compared with LPS-stimulated microglia in the absence of IL-17. The data represent typical samples performed in triplicate in three independent experiments.

using a microtiter plate reader. Nitrite concentrations were calculated from a $NaNO_2$ standard curve.

2.5. Production of IL-17 by glial cells

Microglia and astrocytes were cultured for 72 h in 6-well plates at a concentration of 1×10^6 cells/ml with various doses of IL-23 (1–100 ng/ml). The culture supernatants were then collected and stored at −80°C until they were assessed. IL-17 production was measured using an ELISA kit specific for murine IL-17 (R&D). Total cellular RNA was extracted from the remaining cells using an RNase Mini Kit (Qiagen). cDNAs encoding mouse IL-17 were amplified using RT-PCRs as described above and the specific primers shown in Table 1. In some experiments, cytoplasmic levels of IL-17 in the microglia were also assessed as follows: stimulated microglial cultures were washed four times in cold PBS, the cells were lysed using sonication in ice-cold PBS containing protease inhibitors (complete mini EDTA-free; Roche, Mannheim, Germany), and the lysates were assayed for cellular IL-17 using ELISAs.

3. Results

3.1. Expression of the IL-17 receptor

Increased levels of IL-17 have been observed in the cerebrospinal fluid from patients with active MS as well as in the CNS of EAE mice. Thus, we assessed the expression of IL-17 receptor in CNS cells. RT-PCR demonstrated that neonatal microglia and astrocytes along with splenic T cells and peripheral macrophages expressed IL-17 receptor mRNA, whereas embryonic neurons did not (Fig. 1). Western blot analysis demonstrated that neonatal microglia and astrocytes along with splenic T cells and peripheral macrophages expressed IL-17 receptor protein, whereas embryonic neurons did not (Fig. 1).

We next compared the expression of IL-17 receptor mRNA and protein in adult brain with that of neonatal brain. The expression of mRNA for IL-17 receptor in adult brain was lower than that of neonatal, but protein level of IL-17 receptor was almost identical in these 2 samples (Fig. 1, left panel).

3.2. Effects of IL-17 on microglia

We then assessed the effects of IL-17 on microglia. IL-17 induced the mRNA expression of the inflammatory cytokines IL-6 and MIP-2 with maximum induction observed at 10 ng/ml (Fig. 2A). IL-17, however, did not significantly induce the expression of mRNA encoding IL-1β or TNFα. Upregulation of the expression of IL-6 and MIP-2 protein by IL-17 was confirmed with ELISAs; IL-17 at a concentration of 10 ng/ml or greater significantly increased the production of IL-6 and MIP-2 by microglia (Fig. 2B), whereas IL-1β and TNFα were not detected in the supernatants (data not shown). Although IL-17 by itself did not induce the expression of iNOS mRNA and NO production in unstimulated microglia, it enhanced iNOS mRNA expression and NO production in LPS-stimulated microglia; the maximum increase was observed with 10 ng/ml IL-17 (Fig. 3). In addition, IL-17 dose-dependently upregulated the expression of neurotrophic factors NGF, BDNF, and GDNF (Figs. 4 and 5). IL-17 itself did not induce the expression of mRNA encoding class II major histocompatibility complex (MHC) antigen or cell adhesion molecules (data not shown). On the other hand, the expression of intercellular adhesion molecule (ICAM)-1 and vascular cell adhesion molecule (VCAM)-1 mRNA was upregulated in INFγ-stimulated microglia following treatment with IL-17, whereas it did not affect the expression of class II MHC antigen in these cells (Fig. 6). In contrast to the proinflammatory effects, IL-17 increased the expression of neurotrophic factors in microglia, which may contribute to anti-inflammatory defense mechanisms in the CNS and implies that microglia have multiple functions.

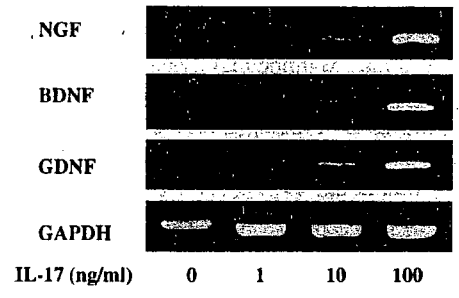

Fig. 4. The effects of IL-17 on the expression of mRNA coding for neurotrophic factors in microglia. Microglia were treated with IL-17 for 72 h. IL-17 dose-dependently induced the expression of NGF, BDNF, and GDNF mRNA.

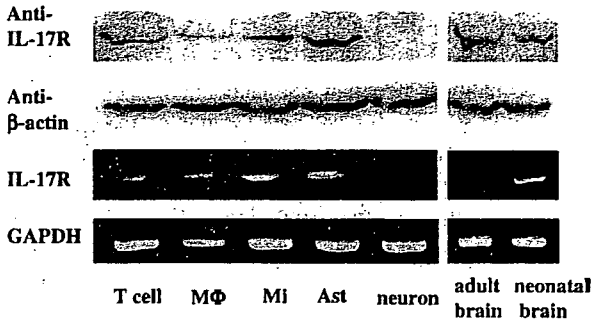

Fig. 1. Expression of IL-17 receptor mRNA and protein in neural cells. Microglia and astrocytes along with splenic T cells and macrophages express IL-17 receptor mRNA and protein, whereas neurons do not. MΦ, macrophages; Mi, microglia; Ast, astrocytes (left panel). The mRNA expression of IL-17 receptor in adult brain was lower than that of neonatal, but protein level of IL-17 receptor was the same as neonatal (right panel).

1:5000 dilution of peroxidase-conjugated, anti-rat IgG secondary antibody (Amersham Bioscience) followed by an additional rinse. IL-17 receptor was detected by ECL (Amersham Bioscience). The molecular weight of IL-17 receptor was determined by running molecular weight markers (Invitrogen) in an adjacent lane. Spleen cells served as a positive control.

2.4. Effects of IL-17 on the production of cytokines, neurotrophic factors and NO by microglia

Microglia and astrocytes were cultured in 24-well plates at a concentration of 1×10^6 cells/ml with or without 1 μg/ml LPS for 24 to 72 h in presence of various doses of IL-17 (1–100 ng/ml). The supernatants were then collected and stored at −80 °C until they were assessed. Total cellular RNA was extracted from remaining cells using an RNase Mini Kit (Qiagen). cDNAs encoding mouse TNFα, IL-1β, IL-6, iNOS, MIP-2 (the functional analogue of human IL-8), Nerve growth factor (NGF), glial cell line-derived neurotrophic factor (GDNF), brain-derived neurotrophic factor (BDNF) and IL-17 were generated and amplified in RT-PCRs as described above using the specific primers shown in Table 1.

Cytokine production was measured using ELISA kits specific for TNFα, IL-6 (Techne), MIP-2, and IL-17 (R&D).

Cellular levels of NGF and BDNF in the microglia were also assessed as follows: stimulated microglial cultures were washed four times in cold PBS, the cells were lysed using sonication in ice-cold PBS containing protease inhibitors (complete mini EDTA-free; Roche, Mannheim, Germany), and the lysates were assayed for cellular NGF and BDNF using ELISA kits specific for NGF and BDNF (Promega, WI, USA). Cytoplasmic GDNF content was measured by an enzyme immunoassay (EIA) as described (Nitta et al., 1999). The EIA system for GDNF was based on the method originally developed for the EIA of NGF, BDNF, and NT-3 (Furukawa et al., 1983; Kaechi et al., 1993; Nitta et al., 1999; Nitta et al., 2004). Antibodies against GDNF were produced by immunizing rabbits with purified human recombinant GDNF. GDNF protein (0.5 mg) in phosphate-buffered saline (PBS; 5 ml) was emulsified with an equal volume of Freund's adjuvant and injected intradermally into rabbits four times at 2-week intervals. Animals were exsanguinated 1 week after the final injection. To affinity purify the antibody, antiserum (1 ml) first was loaded onto a GDNF-linked column (1-ml bed volume; Affi-Gel 10; Bio-Rad, Hercules, CA). After extensive sequential washing with three buffers, 0.1 M Tris–HCl (pH 7.4) containing 0.9% NaCl, 0.05 M borate buffer (pH 8.0), and 0.05 mM sodium acetate buffer (pH 5.0), the bound antibodies were eluted with a 0.1 M glycine–HCl buffer (pH 2.0). A part of the purified anti-GDNF antibody preparation was eluted and biotinylated. The detection limit of the EIAs was as low as 1 pg/ml.

NO production was determined using the Griess reaction as described (Pollock et al., 1991). Briefly, 50-μl aliquots of the supernatants were mixed with an equal volume of Griess reagent (0.1% *N*-ethylenediamine dihydrochloride, 1% sulfanilamide, and 2.5% phosphoric acid) and incubated for 5 min at room temperature. The absorbance at 540 nm was measured

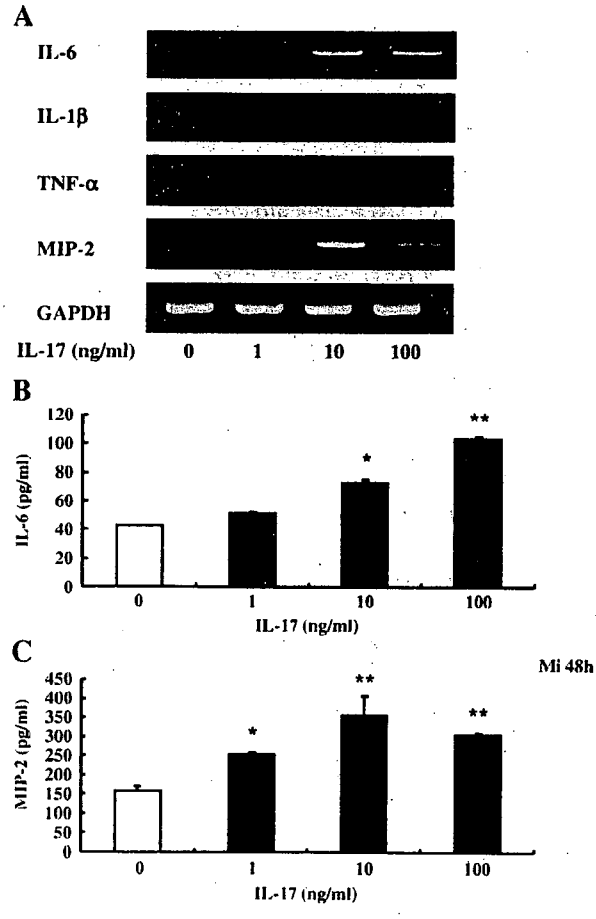

Fig. 2. The effects of IL-17 on cytokine production by microglia. Microglia were treated with IL-17 for 48 h. (A) At concentrations greater than 1 ng/ml, IL-17 induced the expression of IL-6 and MIP-2 mRNA. Similar results were obtained for IL-6 (B) and MIP-2 (C) protein using specific ELISAs. The values shown are the means±S.D. $^*P<0.05$ and $^{**}P<0.01$ compared with untreated microglia. The data represent typical samples performed in triplicate in three independent experiments.

IL-17 levels have been shown to be significantly higher in the cerebrospinal fluid of patients with active optico-spinal MS (Ishizu et al., 2005) and in the CNS of EAE mice (Hofstetter et al., 2005). The effects of IL-17 on CNS cells, however, are unclear. In order to uncover the contribution of IL-17 to inflammatory demyelination in the CNS, we have examined the effects of IL-17 on microglia, which function as antigen-presenting cells and effector cells in the CNS during inflammatory demyelination.

2. Materials and methods

2.1. Reagents

Lipopolysaccharide (LPS), human recombinant transforming growth factor (TGF)-β, and mouse recombinant IL-17 and IL-23 were obtained from Sigma-Aldrich (St. Louis, MO, USA). Mouse recombinant IL-1β, TNFα, and IFNγ were purchased from Techne (Minneapolis, MN, USA). Sulfonylamide, *N*-(1-naphthyl)ethylenediamine, and phosphate for Griess reagent (Ignarro et al., 1987) were also purchased from Sigma-Aldrich.

2.2. Cell culture

The protocols for the animal experiments were approved by the Animal Experiment Committee of Nagoya University. All primary cultures were prepared from C57BL/6J mice (Japan SLC, Hamamatsu, Shizuoka, Japan). Microglia were isolated from primary mixed glial cell cultures prepared from newborn mice on day 14 using the "shaking off" method as previously described (Suzumura et al., 1987); the purity of the cultures was almost 100%, as determined by immunostaining with anti-CD11b antibodies. The cultures were maintained in Dulbecco's modified Eagle's minimum essential medium (Sigma-Aldrich) supplemented with 10% fetal calf serum (JRH Biosciences, Lenexa, KS, USA), 5 μg/ml bovine insulin (Sigma), and 0.2% glucose.

Astrocyte-enriched cultures were prepared as described previously (Kuno et al., 2006). Briefly, the mixed glial cell cultures were trypsinized after the microglia were collected, and replated in Petri dishes. After this procedure was repeated three times, the cultures that had undergone four passages were used as the astrocyte-enriched cultures. The purity of the cultures were more than 80% as determined by immunostaining with anti-glial fibrillary acidic protein (GFAP). Peritoneal macrophages were collected from mice intraperitoneally injected with thioglycolate 48 h prior to collection. T cell-rich lymphocytes were separated from mouse spleens. Neuronal cultures were prepared from mice at embryonic day 17 as described previously (Takeuchi et al., 2005). Briefly, cortices were dissected and freed of meninges. Cortical fragments were dissociated into single cells using dissociation solution, and they were resuspended in Nerve-Cell Culture Medium (serum-free conditioned medium from 48-h rat astrocyte confluent cultures based on Dulbecco's modified Eagle's minimum essential medium/F-12 with N2 supplement, Sumitomo Bakelite, Akita, Japan). The purity of the cultures was more than 95% as determined by NeuN-specific immunostaining.

2.3. Expression of IL-17 receptors

The mRNA expression of the IL-17 receptor was examined using reverse transcription-polymerase chain reactions (RT-PCRs). Microglia, astrocytes, or neurons were cultured for 3 days before total cellular RNA was extracted using an RNase Mini Kit (Qiagen). cDNA encoding the IL-17 receptor was examined by RT-PCR analysis using SuperScript II (Invitrogen), AmpliTaq DNA polymerase (Applied Biosystems), and the specific primers shown in Table 1. Amplification within the linear range using 5 μl of each cDNA sample was achieved following 30 cycles in a DNA thermal cycler under conditions that were optimized for each set of primers.

The protein level of IL-17 receptor expression was examined using Western blot analysis. Samples (20 μg/well) were electrophoresed on 7.5% SDS-polyacrylamide gels (Invitrogen) according to the Laemmli method (Laemmli and Favre, 1973). After electrophoresis, proteins were transferred from the gels to nitrocellulose membranes (Amersham Bioscience, Buckinghamshire, UK) using standard procedures (Towbin et al., 1979). Nonspecific binding was blocked with 5% nonfat dry milk in TBST buffer (5 mM Tris–HCl, pH 7.6, 136 mM NaCl, 0.05% Tween 20) for 1 h. Blots were incubated for 12 h at 4 °C with rat anti-mouse IL-17 receptor antibody (R&D Systems) (1:1000 dilution). Blots were washed four times in TBST: the first time for 20 min and 10 min each time thereafter. We then incubated the washed blots for 1 h at room temperature with a

Table 1
Primer sequences used for RT-PCR analysis

GAPDH sense, 5′-ACTCACGGGAAATTCAACG
GAPDH antisense, 5′-CCCTGTTGCTGTAGCCGTA
IL-17R sense, 5′-CTAAACTGCACGGTCAAGAAT
IL-17R antisense, 5′-ATGAACCAGTACACCCAC
TNFα sense 5′-ATGAGCACAGAAAGCATGATCCGC
TNFα antisense 5′-CCAAAGTAGACCTGCCCGGACTC
IL-1β sense, 5′-ATGGCAACTGTTCCTGAACTCAACT
IL-1β antisense, 5′-CAGGACAGGTATAGATTCTTTCCTTT
IL-6 sense, 5′-ATGAAGTTCCTCTCTGCAAGAGACT
IL-6 antisense, 5′-CACTAGGTTTGCCGAGTAGGATCTC
MIP-2 sense, 5′-CCGGCTCCTCAGTGCTG
MIP-2 antisense, 5′-GGTCAGTTAGCCTTGCCTTT
IL-17 sense, 5′-CAGGACGCGCAAAACATGA
IL-17 antisense, 5′-GCAACAGCATCAGAGAGACACAGAT
iNOS sense, 5′-CCCTTCCGAAGTTTCTGGCAGCAGC
iNOS antisense, 5′-GGCTGTCAGAGCCTCGTGGCTTTGG
NGF sense, 5′-CATAGCGTAATGTCCATGTTGTTCT
NGF antisense, 5′-CTTCTCATCTGTTGTCAACGC
BDNF sense, 5′-AGCCTCCTCTGCTCTTTCTG
BDNF antisense, 5′-TTGTCTATGCCCCTGCAGCC
GDNF sense, 5′-ATTTTATTCAAGGCCACCATTA
GDNF antisense, 5′-GATACATCCACACCGTTTTAGC
MHC class II antigen sense, 5′-AAGAAGGAGACTGTCTGGATGC
MHC class II antigen antisense, 5′-TGAATGATGAAGATGGTGCCC
ICAM-1 sense, 5′-TTCACACTGAATGCCAGCTC
ICAM-1 antisense, 5′-GTCTGCTGAGACCCCTCTTG
VCAM-1 sense, 5′-ATTTTCTGGGGCAGGAAGTT
VCAM-1 antisense, 5′-ACGTCAGAACAACCGAATCC

Please cite this article as: Kawanokuchi, J. et al., Production and functions of IL-17 in microglia, J. Neuroimmunol. (2007), doi:10.1016/j.jneuroim.2007.11.006

ELSEVIER

Journal of Neuroimmunology xx (2007) xxx–xxx

Journal of Neuroimmunology

www.elsevier.com/locate/jneuroim

Production and functions of IL-17 in microglia

Jun Kawanokuchi [a], Kouki Shimizu [a], Atsumi Nitta [b], Kiyofumi Yamada [b], Tetsuya Mizuno [a], Hideyuki Takeuchi [a], Akio Suzumura [a,*]

[a] *Department of Neuroimmunology, Research Institute of Environmental Medicine, Nagoya University, Furo-cho, Chikusaku, Nagoya 464-8601, Japan*
[b] *Department of Neuropsychopharmacology and Hospital Pharmacy, Nagoya University Graduate School of Medicine Showa-ku, Nagoya 466-8560, Japan*

Received 26 July 2007; received in revised form 16 November 2007; accepted 19 November 2007

Abstract

Interleukin (IL)-17-producing helper T cells may play a pivotal role in the pathogenesis of multiple sclerosis. Here, we examined the effects of IL-17 on microglia, which are known to be critically involved in multiple sclerosis. Treatment with IL-17 upregulated the microglial production of IL-6, macrophage inflammatory protein-2, nitric oxide, adhesion molecules, and neurotrophic factors. We also found that IL-17 was produced by microglia in response to IL-23 or IL-1β. Because microglia produce IL-1β and IL-23, these cytokines may act in an autocrine manner to induce IL-17 expression in microglia, and thereby contribute to autoimmune diseases, such as MS, in the central nervous system.

Keywords: Cytokine; IL-17; EAE; MS; Microglia

1. Introduction

Multiple sclerosis (MS) is a chronic inflammatory demyelinating disorder that affects the central nervous system (CNS). Although the etiology of MS is not fully understood, T helper 1 (Th1) cells and the cytokines that they produce are thought to play a role in the development of MS. Recently, interleukin (IL)-17 producing helper T (Th17) cells play important roles in the induction of autoimmune diseases including MS and the corresponding animal model—experimental autoimmune encephalomyelitis (EAE) (Hofstetter et al., 2005, Ishizu et al., 2005, Iwakura and Ishigame, 2006). It has been shown that IL-17 mRNA levels are high in both the cerebrospinal fluid and plaques of MS patients (Matusevicius et al., 1999, Lock et al., 2003). IL-17 is a T cell-derived proinflammatory molecule that stimulates epithelial, endothelial, and fibroblastic cells to produce other inflammatory cytokines and chemokines, including IL-6, macrophage inflammatory protein (MIP)-2, granulocyte-colony stimulating factor (G-CSF), and monocyte chemoattractant protein (MCP)-1 (Aggarwal and Gurney, 2002; Yao et al., 1995; Kennedy et al., 1996; Fossiez et al., 1996; Linden et al., 2000; Cai et al., 1998; Jovanovic et al., 1998; Laan et al., 1999). IL-17 also synergizes with other cytokines such as tumor necrosis factor (TNF)α and IL-1β to further induce chemokine expression (Jovanovic et al., 1998; Chabaud et al., 1998). Although the precise mechanisms that control Th17 cell development have yet to be elucidated, Th17 cells are thought to develop from naïve T helper (Th0) cells via a pathway that is different than the pathways that lead to the development of Th1 and Th2 cells. In the absence of interferon (IFN)γ and IL-4, IL-23 has been shown to maintaining Th17 phenotype in a manner that is not dependent on the transcription factors STAT1, T-bet, STAT4, and STAT6 (Aggarwal et al., 2003; Harrington et al., 2005; Park et al., 2005; Bettelli et al., 2006). Interestingly, a recent study revealed that IL-27 is a critical regulator of IL-17 production. IL-27 receptor-deficient mice were found to generate more IL-17-producing T helper cells and were hypersusceptible to EAE, suggesting that IL-27 negatively regulates the development of Th17 cells (Batten et al., 2006).

* Corresponding author. Department of Neuroimmunology, Research Institute of Environmental Medicine, Nagoya University, Furo-cho, Chikusaku, Nagoya 464-8601, Japan. Tel.: +81 52 789 3881; fax: +81 52 789 3885.
E-mail address: suzumura@riem.nagoya-u.ac.jp (A. Suzumura).

0165-5728/$ - see front matter © 2007 Elsevier B.V. All rights reserved.
doi:10.1016/j.jneuroim.2007.11.006

Available online at www.sciencedirect.com
ScienceDirect
Journal of Nutritional Biochemistry xx (2007) xxx–xxx
Journal of Nutritional Biochemistry

Allicin inhibits cell growth and induces apoptosis through the mitochondrial pathway in HL60 and U937 cells

Talia Miron[a,*], Meir Wilchek[a], Ayala Sharp[b], Yoshihito Nakagawa[c], Makoto Naoi[c], Yoshinori Nozawa[c], Yukihiro Akao[c]

[a]Department of Biological Chemistry, Weizmann Institute of Science, Rehovot 76100, Israel
[b]Department of Biological Services, Weizmann Institute of Science, Rehovot 76100, Israel
[c]Gifu International Institute of Biotechnology, Kakamigahara, Gifu 504-0838, Japan

Received 22 April 2007; received in revised form 12 June 2007; accepted 20 June 2007

Abstract

In this article, the effects of allicin, a biological active compound of garlic, on HL60 and U937 cell lines were examined. Allicin induced growth inhibition and elicited apoptotic events such as blebbing, mitochondrial membrane depolarization, cytochrome *c* release into the cytosol, activation of caspase 9 and caspase 3 and DNA fragmentation. Pretreatment of HL60 cells with cyclosporine A, an inhibitor of the mitochondrial permeability transition pore (mPTP), inhibited allicin-treated cell death. HL60 cell survival after 1 h pretreatment with cyclosporine A, followed by 16 h in presence of allicin (5 μM) was ~80% compared to allicin treatment alone (~50%). Also *N*-acetyl cysteine, a reduced glutathione (GSH) precursor, prevented cell death. The effects of cyclosporine A and *N*-acetyl cysteine suggest the involvement of mPTP and intracellular GSH level in the cytotoxicity. Indeed, allicin depleted GSH in the cytosol and mitochondria, and buthionine sulfoximine, a specific inhibitor of GSH synthesis, significantly augmented allicin-induced apoptosis. In HL60 cells treated with allicin (5 μM, 30 min) the redox state for 2GSH/oxidized glutathione shifted from E_{GSH} −240 to −170 mV. The same shift was observed in U937 cells treated with allicin at a higher concentration for a longer period of incubation (20 μM, 2 h). The apoptotic events induced by various concentrations of allicin correlate to intracellular GSH levels in the two cell types tested (HL60: 3.7 nmol/10^6 cells; U937: 7.7 nmol/10^6 cells). The emerging mechanistic basis for the antiproliferative function of allicin, therefore, involves the activation of the mitochondrial apoptotic pathway by GSH depletion and by changes in the intracellular redox status.

Keywords: Allicin; Apoptosis; Garlic; GSH; HL60; U937

1. Introduction

Allicin, diallyl thiosulfinate, is the main biologically active compound derived from garlic. It is produced by the interaction of the enzyme alliinase (alliin lyase; EC 4.4.1.4) with its substrate alliin (*S*-allyl-L-cysteine sulfoxide) [1]. Since alliinase and alliin are enclosed in different compartments within the garlic clove cells, intact garlic cloves do not contain allicin. When the garlic clove is crushed, alliin and alliinase interact, to form allicin, pyruvic acid and ammonia (Scheme 1). Allicin became an object of interest due to its potential to confer a vast spectrum of health beneficial effects including: anti microbial, antifungal and antiparasitic [2], antihypertensive [3], cardioprotective [4–6], anti-inflammatory [7] and anticancer activities [2,8,9].

In vitro studies of allicin's effect on human mammary MCF-7 cancer cells revealed that its antiproliferative activity is accompanied by accumulation of cells in the regulatory checkpoints, G_0/G_1 and G_2/M, of the cell cycle [9]. Interestingly, also other ally sulfur compound cause similar effects [10]. Allicin was shown to induce apoptosis in gastric

Abbreviations: BSO, D,L-buthionine *S,R*-sulfoximine; CsA, Cyclosporin A; DTNB, 5,5′-dithiobis-(2-nitrobenzoic acid); GGCS, γ-Glutamyl-L-cysteine synthetase; GSH, Reduced glutathione; GSSA, *S*-allylmercaptoglutathione; GSSG, Oxidized glutathione; mPTP, Mitochondrial permeability transition pore; NAC, *N*-acetyl-L-cysteine; XTT, 2,3-Bis (2-methoxy-4-nitro-5-sulfophenyl)-2*H*-tetrazolium-5-carboxanilide sodium salt.

* Corresponding author. Tel.: +972 8 9343627; fax: +972 8 9468256.
E-mail address: talia.miron@weizmann.ac.il (T. Miron).

0955-2863/$ – see front matter © 2007 Published by Elsevier Inc.
doi:10.1016/j.jnutbio.2007.06.009

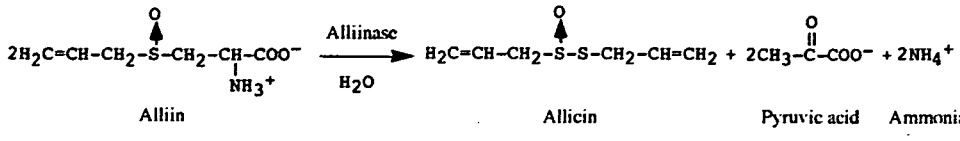

Scheme 1.

cancer SGC-7901 cells. The cause of apoptosis was related to decreased telomerase activity, an enzyme which allicin inhibits in a time- and dose- dependent manner [11]. Allicin induces apoptosis in human cervical cancer SiHa cells and mouse fibroblast-like L-929 cells, manifested through the appearance of characteristic apoptotic morphological changes in apoptotic bodies, through DNA fragmentation, and activation of caspases 8, 9 and 3 [12]. Allicin was also shown to induce apoptosis in human epithelial carcinoma through a caspase-independent pathway, mediated by the release of apoptotic-inducing factor (AIF) from mitochondria and protein kinase A (PKA) activation [13]. More results describing the effects of allicin or other garlic-derived products on various proteins participate in the apoptotic process have already been reported [14]. However, the mechanism underlying the induction of cell death by allicin has not been fully elucidated.

Apoptosis is an ordered cascade of events that culminates in cell death. Two main pathways of apoptosis have been characterized. The extrinsic pathway is initiated through ligand stimulation of the cell surface death receptors such as TNFR or CD95R. In this pathway, cell death is executed via a cascade of proteolytic events with the sequential activation of caspase 8 and caspase 3. The intrinsic pathway is triggered by mitochondrial stress caused by various factors such as DNA damage, oxidative stress and heat shock (reviewed [15]). This pathway is initiated through the release of signal factors from mitochondria as a consequence of mitochondrial membrane permeability transition. Such changes lead to translocation of pro- and antiapoptotic proteins across the mitochondrial membranes [16,17]. Among these proteins is cytochrome *c*, which is released from the mitochondria to the cytosol and participates with other molecules in the formation of a complex that activates caspase 9, which in turn activates caspase 3. The activation of these caspases leads to the final fragmentation of nuclear DNA, with the typical apoptotic morphological manifestations.

Allicin easily diffuses through cell membranes (diffusion coefficient 5×10^{-8} cm^2s^{-1}) [18] and exerts its biological effects by reacting with free thiols within the cell. In living cells, reduced glutathione (GSH) is the major free thiol participating in cellular redox reactions and mixed disulfide formation. GSH is therefore the main cellular target of allicin reaction (Scheme 2). Both allicin and its glutathione derivative, *S*-allylmercaptoglutathione (GSSA), can prevent the formation of free radicals. GSSA is similar in this preventive capacity to GSH, both being less effective in this antioxidant activity than allicin [19–21]. Allicin can scavenge the chain-carrying peroxyl radicals of the substrates by transferring its allylic hydrogen to the oxidized substrate. This renders it a stronger antioxidant than its derivatives [22].

Allicin is a short-lived compound, which rapidly reacts with free intracellular thiol groups [18,19,22]. It was found to disintegrate in the blood a few minutes after its administration, both in vitro in human blood [23] and in vivo in rats [24]. Therefore, the therapeutic effect of allicin administered orally may be restricted to targets that are close to the gastrointestinal tract. However, its main oxidation products, *S*-allylmercapto-glutathione and *S*-allylmercapto-cysteine, could exert their action in more remote sites within the body because they are more stable. The rapid disappearance of allicin can be exploited in tumor cells targeting. We previously showed that allicin kills tumor cells in vitro [25,26] and also in vivo if generated on their surface by conjugating alliinase to monoclonal antibodies directed to specific cell-surface receptors, such as ErbB2, overexpressed in breast and ovarian cancer [25]; CD20, a receptor expressed at high levels in human B chronic lymphocytic leukemia and other B-cell lymphomas [26].

The redox environment of a cell reflects the sum of the products of the reduction potential and the reducing capacity of the linked redox couples operating within the cell [27,28] Glutathione is considered to be the major thiol-disulfide redox buffer of cells [29]. The redox state of the 2GSH/ oxidized glutathione (GSSG) redox couple depends on their molar ratio. Upon reacting with GSH, allicin causes a decrease in free GSH concentration and an increase in mixed-disulfide glutathione products, which leads to an increase in the reduction potential values. Allicin also reacts

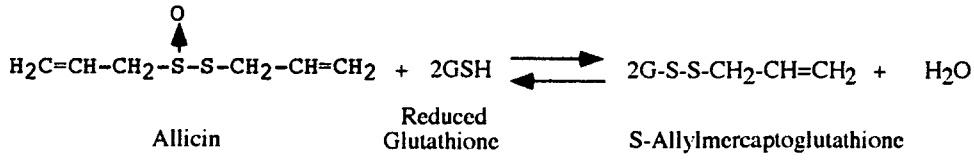

Scheme 2.

with other free SH-bearing molecules in the cell, such as cysteine and SH residues in proteins, yet their relatively low concentrations contribute only little towards changing the reduction potential of the cell upon oxidation. The reduction potential of cells was proposed to reflect their growth cycle. Accordingly, the reduction potential of proliferating cells (pH 7.0) is E_{GSH} −240 mV. Increased values (E_{GSH} −200 mV) represent differentiation, and a further oxidative shift to a higher value (E_{GSH} −170 mV) elicits apoptosis [27]. In this study, we aimed to examine the initial events leading to apoptosis upon allicin treatment and the dependence of the apoptotic pathway on the reduction potential of cells.

2. Materials and methods

Alliin was synthesized from L-cysteine and allyl bromide followed by H_2O_2 oxidation [30]. Allicin (purity ~98%) was produced by applying synthetic alliin onto an immobilized alliinase column and its concentration was determined by high-performance liquid chromatography, as previously described [31].

2,3-Bis (2-methoxy-4-nitro-5-sulfophenyl)-2 *H*-tetrazolium-5-carboxanilide (XTT) sodium salt; D,L-buthionine *S*, *R*-sulfoximine (BSO); cyclosporin A (CsA); *N*-acetyl-L-cysteine (NAC); 5,5′-dithiobis-(2-nitrobenzoic acid) (DTNB); metaphosphoric acid; phenazine methosulfate (PMS) and 2-vinylpyridine were purchased from Sigma Chemical (St. Louis, MO, USA).

2.1. Cell culture, cell viability and morphological studies

HL60 human promyelocytic leukemia-derived cells and U937 human myelomonocytic cells were maintained in RPMI-1640 supplemented with 2 mM L-glutamine, 10% (v/v) fetal bovine serum and antibiotics. Cell viability was measured using the XTT assay, based on the reduction of tetrazolium salt to soluble formazan compounds by mitochondrial enzymes. Cells (15,000–20,000 cells/well) were seeded in a 96-well plate. After 16-h incubation with allicin, in the presence or absence of NAC (0.1–1.0 mM) or after 16 h incubation with BSO (0.1 mM) alone, 50 μl of XTT/PMS mixture (50 μM PMS, 0.1% XTT in medium) were added onto the cells. After an incubation period of 3–4 h at 37°C, the absorbance of the samples was measured in an enzyme-linked immunosorbent assay (ELISA) reader at 450 nm. SDS (1%, 10 μl/well) was added to reference wells before adding the XTT/PMS solution.

HL60 cells (300,000/ml) were pretreated with CsA for 1 h. Cells were seeded in a 96-well plate (20,000 cells/well) in the presence of allicin. The viability was tested by the XTT assay. The analysis of apoptotic morphological changes was done by staining cells with Hoechst 33342 at 37°C for 30 min in medium, washing with phosphate-buffered saline (PBS) and examining by fluorescence microscopy. For evaluating DNA ladder formation, cellular DNA was extracted from cells by ethanol precipitation of the phenol/chloroform extract [32]. After electrophoresis (5–10 μg DNA/lane) on an agarose (2.5%) gel, DNA was visualized by ethidium bromide staining.

Mitochondrial membrane potential was measured by using the fluorescent dye, Mito Tracker Red CMXRos (Molecular Probes, Eugene, OR, USA) that accumulates selectively in active mitochondria. Cells were washed with medium, incubated with Mito-Tracker Red CMXRos for 30 min at 37°C, washed with PBS and examined under fluorescence microscopy (Olympus, Tokyo).

Mitochondria were prepared from cultured cells (5–10×10^7) as described elsewhere [33]. Cells were harvested and washed with PBS (600 g, 7 min). Cell pellets were suspended in 0.5 ml cold HIM buffer (200 mM mannitol, 70 mM sucrose, 1 mM EGTA, 10 mM HEPES-KOH buffer, pH 7.5) containing protease inhibitors, incubated 30 min on ice and homogenized by multiple passages through a 25-gauge needle (5/8 in.). Nuclei and unbroken cells were removed (1300 g, 8 min at 4°C). Protein and free SH were determined in the cytosol, supernatant (10,000 g, 30 min at 4°C) and in the mitochondria-enriched fraction (pellet, dissolved in HIM buffer containing 1% Triton X-100). Protein assay was done with the Biuret Reagent [34] or the BCA protein assay kit (Pierce, Rockford, IL, USA).

2.2. Cell cycle analysis

HL60 cells were pretreated with CsA (5 μM, 1 h) and then cultured further for 20 h in the presence or absence of allicin. After harvesting, washing and resuspending in 0.25 ml PBS, an equal volume of 0.005% propidium iodide solution containing 0.01% heated-RNase A and 0.3% Triton X-100 was added. Cells were analyzed by flow cytometry using fluorescence-activated cell sorting (Becton Dickinson FACScan Instrument using CellQuest software (BD Bioscience, San Jose, CA, USA).

2.3. Electrophoresis and Western blot analysis

Cell pellet was resuspended in lysis buffers A or B [32]. Lysis buffer A (2×PBS, 0.1% sodium dodecyl sulfate (SDS), 1% Nonidet P-40, 0.5% sodium deoxycholate) containing protease inhibitors was used to analyze of caspases 3, 8 and 9. Lysis buffer B (250 mM sucrose, 20 mM HEPES-KOH buffer, pH 7.5, 10 mM KCl, 1.5 mM $MgCl_2$, 1 mM EDTA, 1 mM EGTA, 1 mM DTT) containing protease inhibitors was used to analyze the presence of cytochrome *c* in the cytosol as described above (Section 2.2), After centrifugation (10,000*g*, 30 min, 4°C) the supernatant was separated by SDS-polyacrylamide gel electrophoresis using 15% gel and transferred electrophoretically onto a PVDF membrane (Du Pont, Boston, MA, USA). The membrane was incubated overnight at 4°C with the following antihuman antibodies: anti β-actin (Sigma–Aldrich), anti-caspase 3 (Santa Cruz Biotechnology, Santa Cruz, CA, USA), anti-caspase 8 (MBL, Nagoya, Japan), anti caspase-9 (Novus Biological,

Littleton, CO, USA) and anti cytochrome *c* (Upstate Biotechnology, Lake Placid, NY, USA). The membranes were washed with TBST, incubated with HRP-conjugated secondary antibody for 1 h at room temperature and washed with TBST. Proteins were detected with an enhanced ECL detection kit (New England Biolabs) and a chemiluminescence detector (LAS-1000, Fuji, Japan).

2.4. Determination of cell volume

The volume of nontreated cells was determined by calculating sphere volumes based on diameter measurement of 100 cells. Since the morphology of treated cells was not spherical, cell volume was estimated by weighing the pellet of $2–4\times10^6$ cells and evaluating the volume on the assumption of 1/1 w/v.

2.5. Assay for glutathione and free SH

Cells were collected (600 g, 7 min, 4°C), washed with PBS and the pellets were stored at −80°C. After protein precipitation with 5% metaphosphoric acid (0.2–0.3 ml/3×10^6 cells) by centrifugation (10,000g, for 30 min), the supernatant was used for GSH quantitation, and the pellet, dissolved in 0.2–0.3 ml of 0.5 M NaOH, was used for protein determination. To determine GSH in the supernatant, a glutathione assay kit (Calbiochem) was used. GSH and GSSG content were also determined by the glutathione reductase recycling assay before and after modification with 2-vinyl pyridine [35]. Samples (40 µl) were neutralized with 2 M triethanolamine (10 µl) in a 96-well plate. The reaction was started by adding 200 µl per well of 0.4 U/ml enzyme in 143 mM phosphate buffer pH 7.5 containing 0.3 mM reduced nicotinamide adenine dinucleotide phosphate, 0.6 mM DTNB and 6.25 mM EDTA. The initial rate of 5-thio-2-nitrobenzoic acid formation was monitored. Determination of GSSG was done 1 h after modification of the free SH with 9 M 2-vinyl pyridine (1 µl/well) at room temperature. Oxidized glutathione (0–6 nmol/well) served as a reference.

Total free SH content in cell extracts or in cytosolic and mitochondrial fractions (50 µl) was determined with DTNB in a 96-well plate. Samples were acidified with 5% metaphosphoric acid (50 µl/well) to stabilize the reduced state and neutralized with 2 M triethanolamine (50 µl/well). DTNB (50 µl of 1 mM solution in 50 mM phosphate buffer pH 7.2 containing 2 mM EDTA) was added. After 10 min of incubation, the absorbance was measured at 412 nm using an ELISA reader. GSH (0–20 nmol/well) precalibrated with DTNB served as a reference, using E_M 14150 M^{-1} at 412 nm [36]. Reduction potential was calculated by using the Nernst equation for GSSG/2GSH: $E_{GSH}=E_0-30\times\log([GSH]^2/[GSSG])$ [27].

2.6. Statistical analysis

Each experiment was performed at least three times, and the results were expressed as mean values± S.D. (n=2–6). The Student t test was used to determine the significance of differences between the mean values obtained for the two cell lines. Otherwise, the various treatments, were analyzed using one-way analysis of variance (ANOVA) followed by either Dunnett or Bonferroni's multiple comparison test, considering $P<05$ as significant.

3. Results

3.1. Allicin inhibited proliferation of HL60 and U937 cells

The proliferation rate of exponentially growing HL60 and U937 cells in the presence of allicin was determined at a density of 100,000 cells ml^{-1}. Cells were incubated with increasing concentrations of allicin (HL60: 0–10 µM; U937: 0–30 µM) for growing time periods up to 72 h. Cell viability was determined by the trypan blue dye exclusion assay. Allicin inhibited cell growth in a concentration-dependent manner (Figs. 1A and 2A for HL60 and U937, respectively). In the presence of 5 µM allicin, HL60 cells exhibited about 50% inhibition of proliferation after 22 h, and at 10 µM allicin after 22 h, the rate of inhibition reached 80% (Fig. 1A). HL60 cells were more sensitive to allicin than U937 cells. Inhibition of U937 cell proliferation reached 50% and 60% at 15 and 20 µM allicin, respectively, after 22 h (Fig. 2A). We therefore chose to continue the study of HL60 and U937 cells (100,000 cells/ml) at 5 and 20 µM allicin, respectively.

3.2. Allicin induced apoptosis in the cells

3.2.1. Morphological changes

Morphological changes indicating apoptotic processes were observed by staining the cells with Hoechst 33342. Distinct nuclear condensation was observed in HL60 cells treated with allicin (5 µM) for 16 h (Fig. 1B) and U937 cells treated with allicin (20 µM) for 40 h (Fig. 2B). In both allicin-treated cell lines, more than 90% of the cells showed blebbing after 2 h (Fig. 3A, lower panel).

3.2.2. DNA fragmentation

A DNA ladder appeared in allicin (5 µM)-treated HL60 cells 6 h after treatment, whereas in allicin (20 µM)-treated U937 cells, it appeared only after 40 h (Figs. 1C and 2C).

3.2.3. Cytochrome c release into cytoplasm and activation of caspases

To better understand the mechanism of allicin-induced apoptosis, Western blot analysis was used to detect apoptosis-related proteins. Increased amounts of cytochrome *c* appeared in the cytosol of allicin (5 µM)-treated HL60 cells after 2.5 h of incubation. An increase in cleaved caspase 9 appeared 4 and 6 h after adding allicin, and it gradually decreased to the basal level after 30 h. Cleaved caspase 3 appeared after 16 h and was still observed 30 h after the treatment (Fig. 3B). U937 cells reacted at a slower rate to allicin (20 µM) treatment. Cytochrome *c* release into the cytosol began 6 h after adding allicin and reached a maximal

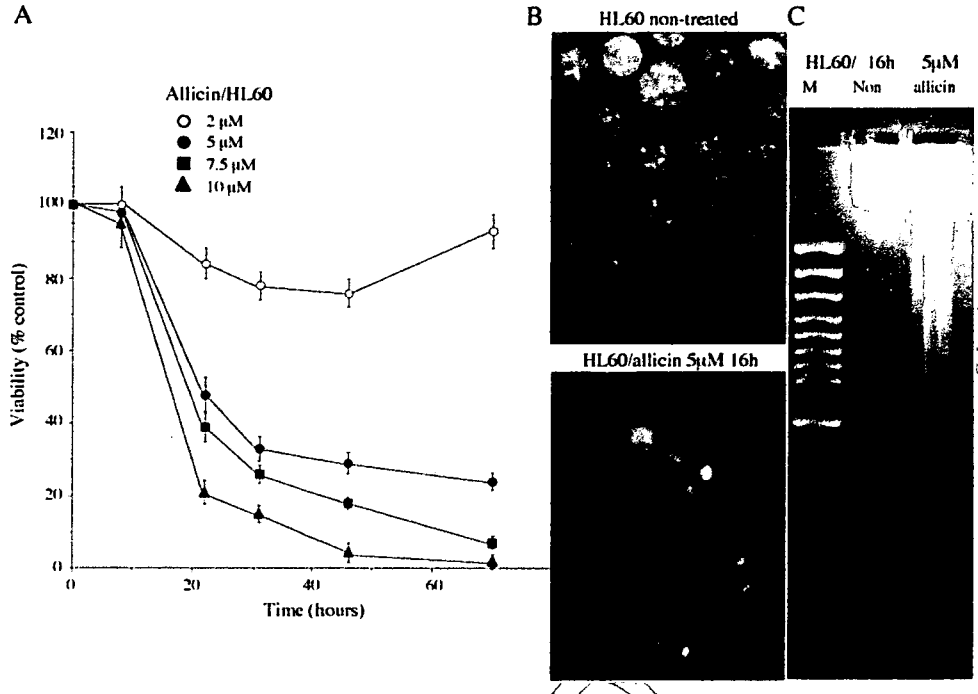

Fig. 1. Effect of allicin on cell growth of human leukemia HL60 cells. (A) Growth dependent of HL60 cells on allicin concentration. Viable cells were counted at various time intervals between 0–72 h after staining with trypan blue. Data represent the mean value of % viable cells (nontreated=100%)±S.D. (B) Apoptotic changes observed after Hoechst 33342 (5 μg/ml) staining for 30 min. Cells were treated with 5 μM allicin for 16 h. (C) Nucleosomal DNA fragmentation of nontreated cells and allicin-treated HL60 cells (5 μM, 6 h, 5 μg/lane). Lane M is a DNA size marker.

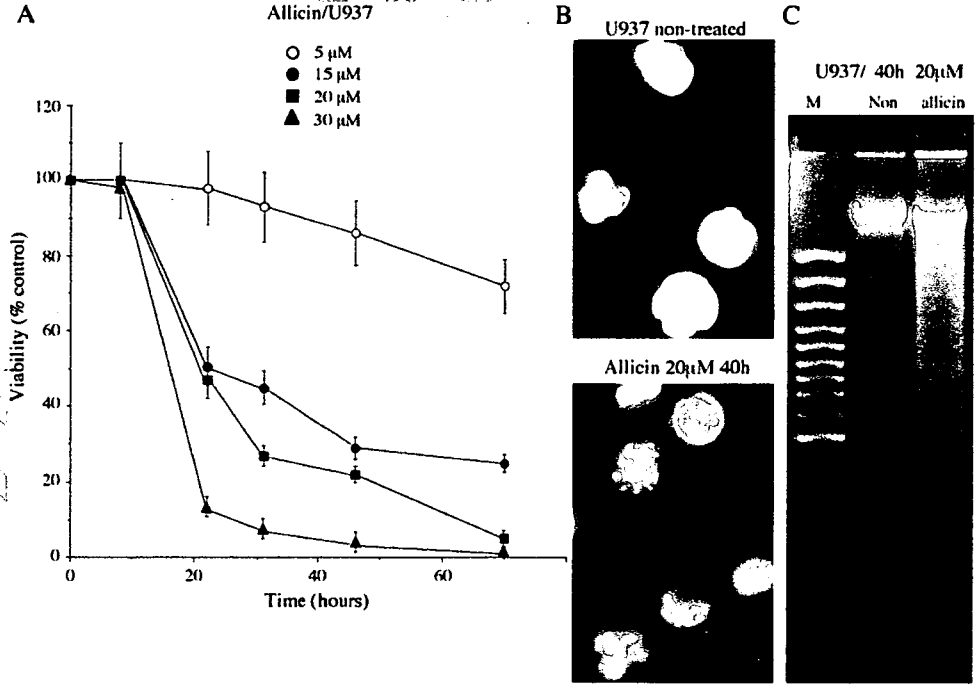

Fig. 2. Effect of allicin on cell growth of human leukemia U937 cells. (A) Growth dependence of U937 cells on allicin concentration. Viable cells were counted at various time intervals between 0–72 h after staining with trypan blue. Data represent the mean value of % viable cells (nontreated=100%)±S.D. (B) Hoechst 33342 (5 μg/ml) staining for 30 min of cells treated with 20 μM allicin for 40 h. (C) Nucleosomal DNA fragmentation of nontreated cells and allicin-treated U937 cells (20 μM, 40 h, 10 μg/lane). Lane M is a DNA size marker.